NASA TECHNICAL NOTE

NASA TN D-7127

NASA TN D-7127

LOCAL HEAT-TRANSFER CHARACTERISTICS OF A ROW OF CIRCULAR AIR JETS IMPINGING ON A CONCAVE SEMICYLINDRICAL SURFACE

by John N. B. Livingood and James W. Gauntner

Lewis Research Center
Cleveland, Ohio 44135

NATIONAL AERONAUTICS AND SPACE ADMINISTRATION • WASHINGTON, D. C. • JANUARY 1973

1. Report No.	2. Government Accession No.	3. Recipient's Catalog No.
NASA TN D-7127		

4. Title and Subtitle	5. Report Date
LOCAL HEAT-TRANSFER CHARACTERISTICS OF A ROW OF CIRCULAR AIR JETS IMPINGING ON A CONCAVE SEMICYLINDRICAL SURFACE	January 1973
	6. Performing Organization Code
7. Author(s)	8. Performing Organization Report No.
John N. B. Livingood and James W. Gauntner	E-7117
	10. Work Unit No.
9. Performing Organization Name and Address	501-24
Lewis Research Center National Aeronautics and Space Administration Cleveland, Ohio 44135	11. Contract or Grant No.
	13. Type of Report and Period Covered
12. Sponsoring Agency Name and Address	Technical Note
National Aeronautics and Space Administration Washington, D. C. 20546	14. Sponsoring Agency Code

15. Supplementary Notes

16. Abstract

An experimental study was made of the local heat-transfer characteristics of air jets impinging on the concave side of a right circular semicylinder. A correlation was developed for expressing individual and combined effects of a number of dimensionless variables on the normalized Nusselt number distributions. Results of the present study are in good agreement with those of other investigators.

17. Key Words (Suggested by Author(s))	18. Distribution Statement
Impinging jets Cylindrical surface Heat-transfer data	Unclassified - unlimited

19. Security Classif. (of this report)	20. Security Classif. (of this page)	21. No. of Pages	22. Price*
Unclassified	Unclassified	25	$3.00

* For sale by the National Technical Information Service, Springfield, Virginia 22151

LOCAL HEAT-TRANSFER CHARACTERISTICS OF A ROW OF CIRCULAR AIR JETS IMPINGING ON A CONCAVE SEMICYLINDRICAL SURFACE

by John N. B. Livingood and James W. Gauntner

Lewis Research Center

SUMMARY

A study of the local heat-transfer characteristics of air jets impinging on the concave side of a right circular semicylinder is reported. The ratios of local to average Nusselt numbers are obtained at various positions along the cooled concave surface and the resulting distributions are compared with others obtained from the literature.

Experimental data reported herein were obtained for nozzles 0.318, 0.635, and 0.952 centimeter (0.125, 0.250, and 0.375 in.) in diameter with center-to-center spacings of 2, 4, and 8 nozzle diameters impinging on a 12.7-centimeter- (5.0-in.-) diameter semicylinder. Nozzle-to-target spacings of 2, 5, and 8 nozzle diameters were considered. Reynolds numbers, based on nozzle diameter, from about 2500 to about 30 000 were investigated.

A method for correlating the normalized Nusselt number distribution against a number of geometrical parameters is presented and evaluated. Results indicate that the effects on the normalized Nusselt number distribution of the ratio of nozzle-to-cylinder diameter and of the ratio of nozzle-to-target spacing to nozzle diameter were significant. On the other hand, the effects of the ratio of nozzle center-to-center spacing to nozzle diameter and of Reynolds number were not significant. Both the correlation and the data from this investigation fell well within the range of results presented in the literature.

INTRODUCTION

Experimentally determined local heat-transfer characteristics for a row of circular turbulent air jets impinging on a concave semicylindrical surface are reported. A method for correlating the ratios of local to average Nusselt numbers against geometrical parameters is also presented and compared to results in the literature.

An effective method of cooling the leading edge region of turbine vanes and blades is by impingement of cool air on the internal surface. Reference 1 presents a review of the available literature on impingement to a concave surface, some experimental average heat transfer data, and suggested correlations for average Nusselt numbers. The purposes of the present report are to augment the results of reference 1 by presenting some experimentally determined local to average Nusselt number ratios and to develop a correlation as a function of dimensionless parameters for these ratios.

The data presented herein were obtained for a row of circular air jets impinging on the internal surface of a semicylinder of diameter 12.7 centimeters (5.0 in.). Air jets of diameters 0.318, 0.635, and 0.952 centimeter (0.125, 0.250, and 0.375 in.) with center-to-center spacings of 2, 4, and 8 nozzle diameters and nozzle-to-target separation distances of 2, 5, and 8 nozzle diameters were considered.

The data were obtained under supervision of Dr. Peter Hrycak at the Newark College of Engineering under NASA Contract NAS3-11175.

SYMBOLS

A	coefficient defined by eq. (2)
A_{sc}	semicylindrical surface area
$A_1, \ldots, A_4$	cylindrical surface area affected by calorimeters 1 to 4
$a_0, \ldots, a_4$	correlation constants in eq. (2)
B	exponent defined by eq. (3)
b_s	equivalent slot width
$b_0, \ldots, b_4$	correlation constants in eq. (3)
c_n	center-to-center nozzle spacing
D	target cylinder diameter
d	nozzle diameter
G	flow rate per unit area
l	half length of target surface measured from stagnation line
Nu_x	local Nusselt number
$\overline{Nu}$	average Nusselt number based on nozzle diameter

$Nu_1, \ldots, Nu_4$	Nusselt numbers related to calorimeters 1 to 4
R	radius of target semicylinder
Re_b	Reynolds number based on equivalent slot width and nozzle exit velocity
Re_d	Reynolds number based on nozzle diameter and nozzle exit velocity
x	surface distance along target measured from stagnation line
z_n	nozzle-to-target separation distance
μ	viscosity

APPARATUS AND PROCEDURE

A schematic diagram of the apparatus is shown in figure 1. Air supplied by a compressor flowed through a filter and oil separator into a large storage tank to provide a

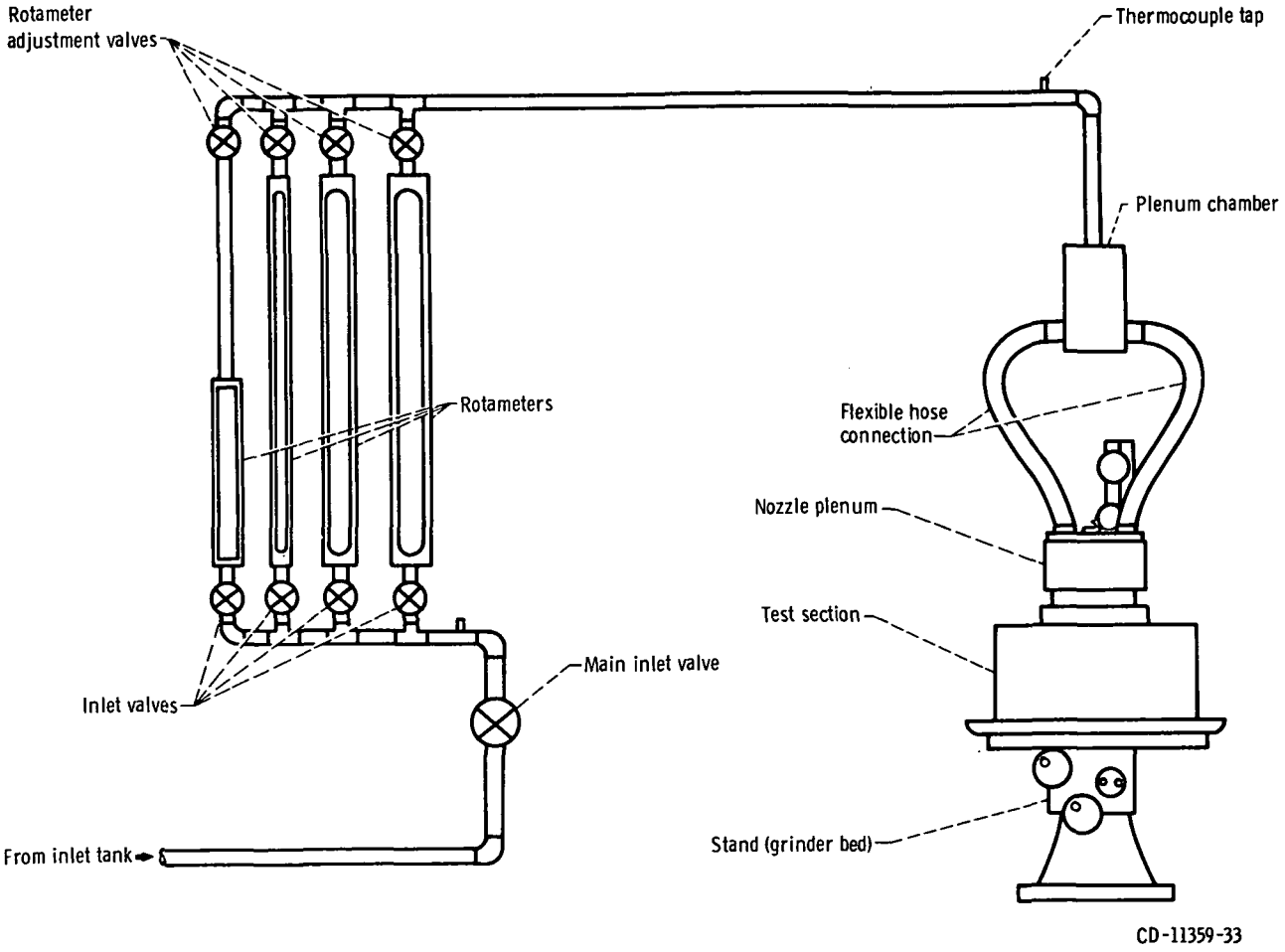

Figure 1. - Schematic of test apparatus.

steady flow. The air flowed through an inlet tank connected to a set of four rotameters in parallel. Depending on the flow rate, the flow was routed through a selected rotameter and into a tube connected to a plenum chamber. The air flowed through two flexible hoses from the plenum chamber into another chamber which contained the row of nozzles through which the air passed to impinge on the test cylinder surface. The test section was secured to a stand made from a grinding machine bed which permitted an accurate alinement of the test section relative to the nozzle chamber.

The rotameters were calibrated within an error of less than 1 percent of full scale. Air pressure was measured at the inlet of the rotameter with a Bourdon-type pressure gage with an assumed accuracy of ±0.34 newton per square centimeter (±0.5 psia). (The inlet valve of the rotameter was kept fully open, and the flow was controlled by adjusting the outlet valve.) The air temperature in the rotameter was measured by a thermocouple placed in the pipe.

Test Assembly

A sketch of the test assembly is shown in figure 2. The semicylindrical target surface was made from a section of a 12.7-centimeter (5.0-in.) diameter 304 stainless

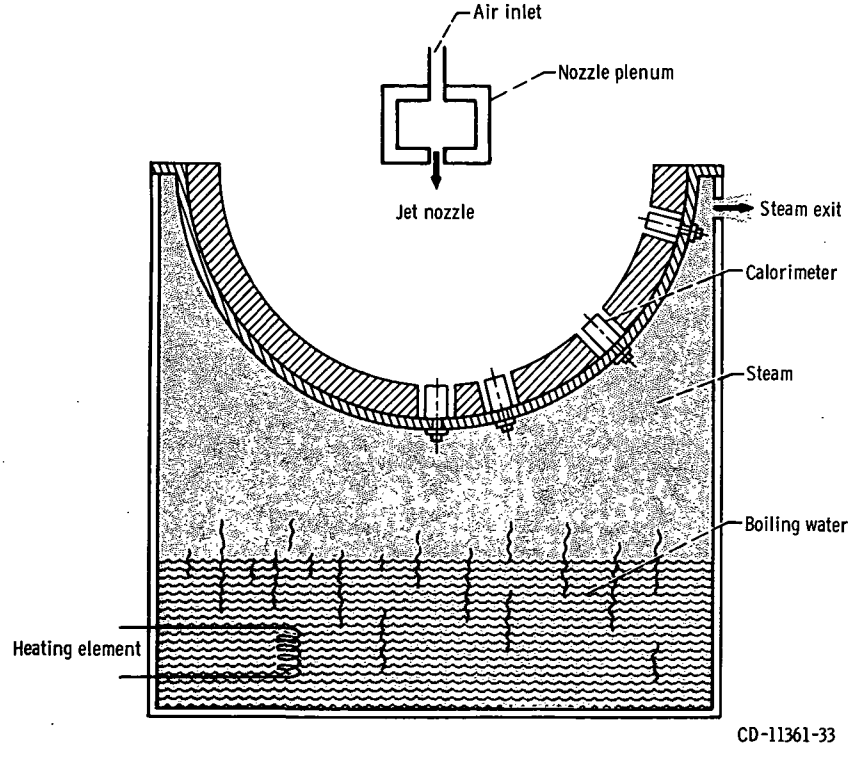

Figure 2. - Test assembly.

steel pipe. The target surface was 25.4 centimeters (10.0 in.) in length and had a nominal wall thickness of 1.14 centimeters (0.45 in.). Both ends of the target surface were blocked with plexiglass sidewalls. The convex surface was supported by a brass plate which was steam heated by placing it over a small tank in which water was kept boiling. To eliminate some of the heat transfer between the air in the nozzle plenum and the exhaust air venting into the room, reflective insulation over a layer of flannel fabric was attached to the nozzle plenum wall. Several layers of plastic air filter material were inserted over an aluminum screen in the nozzle plenum to achieve a more uniform distribution of air.

Twenty-one calorimeters were installed on the target surface as shown in figure 3.

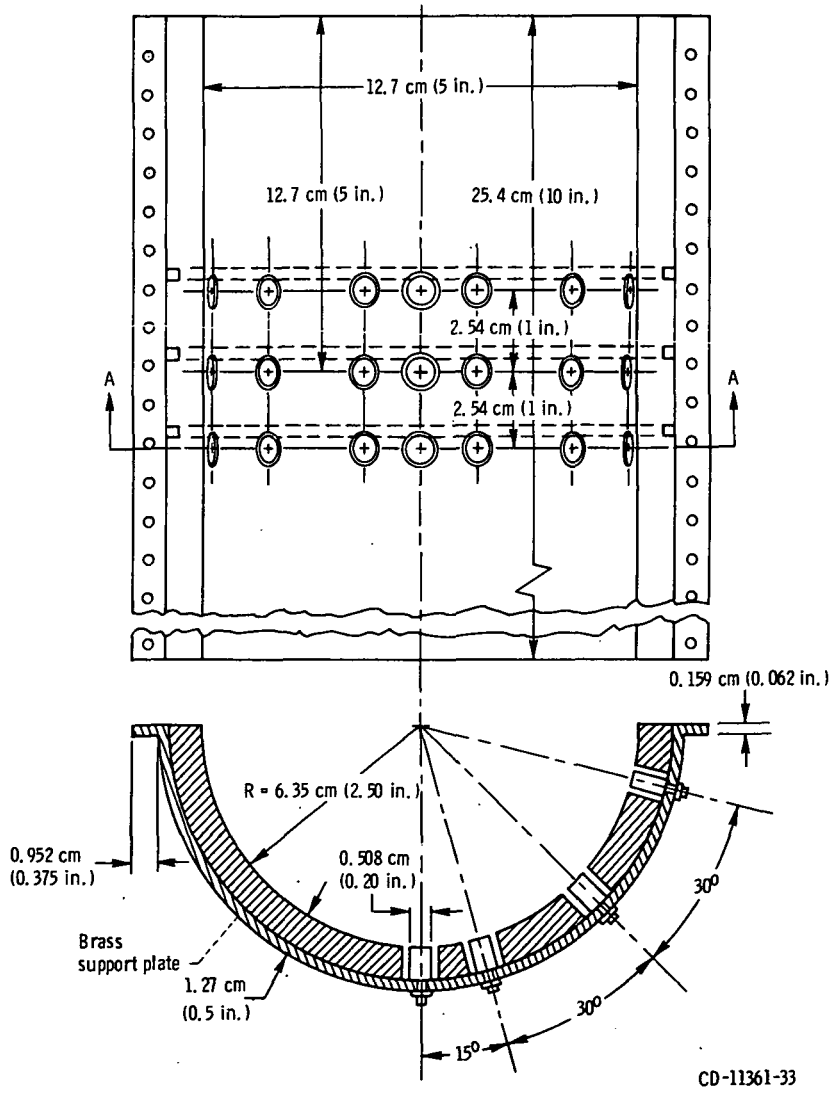

Figure 3. - Calorimeter positions in concave target surface.

The calorimeters were made from the same kind of stainless steel as the target surface and were in the shape of 0.508-centimeter- (0.20-in.-) diameter and 1.143-centimeter- (0.45-in.-) long cylinders with two thermocouples installed 1.016 centimeters (0.40 in.) apart (see fig. 4). The calorimeters were located at three axial positions, at 2.54-centimeter (1.0-in.) spacings; each spanwise position had a calorimeter located at the stagnation line, and at 15°, 45°, and 75° on either side of the stagnation line. In terms of dimensionless distance along the cylinder from the stagnation line, the calorimeters were located at values of $x/l = 0$, 0.167, 0.500, and 0.833.

Nozzles of diameters 0.318, 0.635, and 0.952 centimeter (0.125, 0.250, and 0.375 in.) with center-to-center spacings of 2, 4, and 8 nozzle diameters were considered. The target was mounted on a grinding machine stand which permitted variations in the nozzle-to-target separation distance of 2, 5, and 8 nozzle diameters.

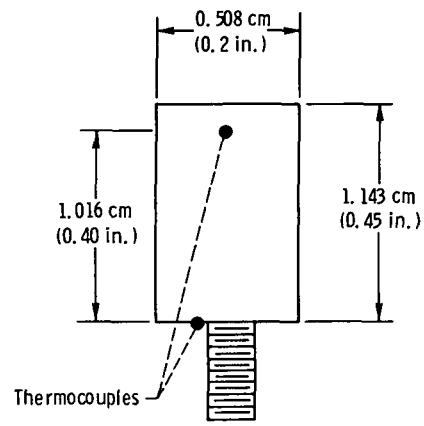

Figure 4. - Calorimeter used to measure heat flux.

Calculation of Nusselt Number Ratios

Stagnation line Nusselt numbers were obtained by averaging experimental data from the three stagnation line calorimeters. Off-stagnation line Nusselt numbers were obtained by averaging the data from the six respective calorimeters for values of $x/l = 0.167$, 0.500, and 0.833. Since the same target surface and calorimeters were used in all tests, some tests were necessarily conducted in which only the stagnation line calorimeter in the center row of calorimeters was alined with an impingement nozzle. Therefore, slight variations in the magnitude of local Nusselt numbers were obtained due to the location of the impingement nozzles relative to the calorimeters. However, the

effect of these variations is minimized when the data are presented in terms of the ratio of local to average Nusselt numbers.

The average Nusselt numbers were obtained as area weighted averages of the local Nusselt numbers. As shown in figure 5, lines were drawn from the center of the cylinder to the points on the cylindrical surface which bisected the arcs between successive

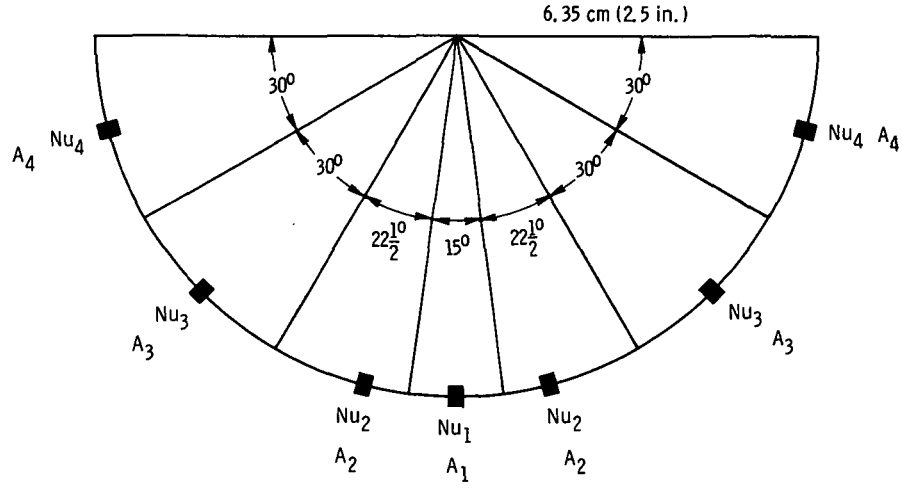

Figure 5. - Semicylindrical breakdown used for determining weighting factors for calculation of average Nusselt numbers.

calorimeters. Associated with each calorimeter was a normalized area obtained by multiplying the respective arc lengths by the length of the cylinder and dividing by the complete semicylindrical surface area. The average Nusselt number was then determined from

$$\overline{Nu} = \frac{Nu_1A_1 + 2Nu_2A_2 + 2Nu_3A_3 + 2Nu_4A_4}{A_{sc}}$$

$$= \frac{Nu_1 + 3Nu_2 + 4Nu_3 + 4Nu_4}{12}$$

where the coefficients have been reduced to their lowest terms.

CORRELATION OF DATA

In order to obtain a correlation for the data presented herein, the effects of the dimensionless variables Re_d, d/D, c_n/d, z_n/d, and x/l on $Nu_x/\overline{Nu}$ must be investigated. Since the dimensionless variable x/l is undoubtedly the predominating variable and since correlations from the literature include the other dimensionless variables (see ref. 1), one is led to investigate the possibility of the use of a correlation such as

$$\frac{Nu_x}{\overline{Nu}} = A\left(\frac{x}{l}\right)^B \tag{1}$$

where

$$A = a_0 \, Re_d^{a_1}\left(\frac{d}{D}\right)^{a_2}\left(\frac{c_n}{d}\right)^{a_3}\left(\frac{z_n}{d}\right)^{a_4} \tag{2}$$

and

$$B = b_0 \, Re_d^{b_1}\left(\frac{d}{D}\right)^{b_2}\left(\frac{c_n}{d}\right)^{b_3}\left(\frac{z_n}{d}\right)^{b_4} \tag{3}$$

Values of the constants a_0 to a_4 and b_0 to b_4 can be found such that equation (1) is a least-squares curve fit through the data.

Although the previous expressions for A and B may satisfy the data, they do not necessarily satisfy the analytical relation that $A = B + 1$. This relation is arrived at by integrating equation (1) for $Nu_x/\overline{Nu}$ over x/l from 0 to 1 and equating the integral to unity. Consequently, for the data considered herein, the exponent B was obtained from a curve fit and the coefficient A was set equal to $B + 1$, yielding the following equation:

$$\frac{Nu_x}{\overline{Nu}} = (B + 1)\left(\frac{x}{l}\right)^B \tag{4}$$

RESULTS AND DISCUSSION

Values of Nu and $Nu_x/\overline{Nu}$ are presented in table I for all cases considered. The

TABLE I. - HEAT-TRANSFER DATA

Dimensionless nozzle-to-target separation distance, z_n/d	Reynolds number based on nozzle diameter and nozzle exit velocity, Re_d	Average Nusselt number based on nozzle diameter, $\overline{Nu}$	Normalized local Nusselt numbers			
			$\frac{Nu_1}{\overline{Nu}}$	$\frac{Nu_2}{\overline{Nu}}$	$\frac{Nu_3}{\overline{Nu}}$	$\frac{Nu_4}{\overline{Nu}}$
Nozzle diameter d = 0.318 cm (0.125 in.); center-to-center nozzle spacing c_n = 2.54 cm (1 in.)						
2	2 690	10.78	3.934	1.051	0.788	0.441
	6 300	17.55	3.630	1.271	.770	.369
	12 710	23.99	3.709	1.279	.776	.341
	27 220	37.06	3.490	1.188	.829	.407
5	2 560	10.68	3.140	1.191	0.877	0.455
	6 040	17.07	2.894	1.190	920	.477
	13 780	25.84	2.998	1.267	.853	.459
	27 240	37.69	2.719	1.201	.927	.492
8	2 870	12.03	2.616	1.238	0.894	0.524
	6 020	17.52	2.367	1.272	.949	.508
	12 660	24.12	2.394	1.216	.926	.563
	26 590	38.11	2.285	1.192	.954	.581
Nozzle diameter d = 0.318 cm (0.125 in.); center-to-center nozzle spacing c_n = 1.27 cm (0.5 in.)						
2	2 640	10.95	3.878	1.010	0.809	0.464
	2 670	11.05	3.889	1.021	.800	.463
	6 600	18.88	3.477	1.135	.811	.469
	6.610	19.28	3.394	1.198	.793	.461
	13 240	29.29	3.182	1.212	.808	.487
	13 240	29.38	3.192	1.211	.808	.486
	26 770	40.80	3.138	1.168	.814	.526
5	2 730	13.78	2.837	1.225	0.874	0.498
	2 770	13.72	2.867	1.221	.864	.493
	6 400	19.44	3.034	1.112	.845	.563
	6 400	19.46	3.036	1.107	.849	.562
	13 330	29.69	2.886	1.124	.856	.580
	13 340	29.78	2.889	1.123	.857	.579
	26 780	40.93	2.903	1.103	.809	.638
	26 790	42.72	2.792	1.059	.894	.614
8	2 840	13.57	2.412	1.133	0.942	0.604
	2 900	13.61	2.402	1.132	.946	.605
	6 290	21.05	2.382	1.115	.951	.617
	6.290	20.47	2.451	1.054	.966	.631

TABLE I. - Continued. HEAT-TRANSFER DATA

Dimensionless nozzle-to-target separation distance, z_n/d	Reynolds number based on nozzle diameter and nozzle exit velocity, Re_d	Average Nusselt number based on nozzle diameter, $\overline{Nu}$	Normalized local Nusselt numbers			
			$\frac{Nu_1}{\overline{Nu}}$	$\frac{Nu_2}{\overline{Nu}}$	$\frac{Nu_3}{\overline{Nu}}$	$\frac{Nu_4}{\overline{Nu}}$
8	13 120	32.52	2.322	1.107	0.944	0.645
	13 120	32.53	2.325	1.115	.940	.642
	26 130	44.83	2.303	.996	.973	.704
	26 640	44.75	2.301	.993	.975	.705
Nozzle diameter d = 0.318 cm (0.125 in.); center-to-center nozzle spacing c_n = 0.635 cm (0.25 in.)						
2	2 790	14.72	3.257	1.059	0.842	0.553
	2 840	14.51	3.256	1.117	.819	.529
	6 510	23.87	3.021	.992	.899	.602
	6 510	23.89	3.024	.990	.899	.603
	12 850	34.04	2.898	.942	.941	.628
	12 920	34.16	2.908	.944	.933	.629
	22 500	44.98	2.829	.977	.907	.658
	22 510	45.01	2.866	.977	.908	.658
5	2 800	15.88	2.606	1.050	0.904	0.656
	2 820	15.85	2.607	1.058	.902	.650
	6 250	26.84	2.434	.978	.946	.712
	6 280	26.77	2.433	.966	.951	.713
	11 460	39.28	2.299	.984	.950	.728
	12 480	39.16	2.303	.985	.945	.730
	22 510	51.96	2.276	.998	.865	.784
	22 510	51.86	2.277	.998	.865	.784
8	2 700	15.47	2.158	1.029	0.951	0.734
	6 030	26.92	1.955	1.032	.931	.781
	6 050	26.24	2.009	.980	.957	.801
	12 560	39.27	1.936	1.068	.898	.775
	12 610	40.12	1.890	1.040	.875	.831
	22 500	54.07	1.810	1.049	.807	.893
	22 680	54.58	1.815	1.049	.804	.894
	30 970	58.93	1.746	.976	.972	.859
Nozzle diameter d = 0.635 cm (0.25 in.); center-to-center nozzle spacing c_n = 5.08 cm (2 in.)						
2	2 666	13.51	2.511	1.366	0.977	0.370
	2 900	13.45	2.611	1.413	.977	.310
	6 147	23.77	2.543	1.549	.938	.265

TABLE I. - Continued. HEAT-TRANSFER DATA

Dimensionless nozzle-to-target separation distance, z_n/d	Reynolds number based on nozzle diameter and nozzle exit velocity, Re_d	Average Nusselt number based on nozzle diameter, $\overline{Nu}$	Normalized local Nusselt numbers			
			$\frac{Nu_1}{\overline{Nu}}$	$\frac{Nu_2}{\overline{Nu}}$	$\frac{Nu_3}{\overline{Nu}}$	$\frac{Nu_3}{\overline{Nu}}$
2	6 348	23.92	2.486	1.549	0.957	0.260
	12 841	39.33	2.320	1.485	.987	.319
	12 844	39.38	2.325	1.486	.984	.321
	26 713	58.02	2.256	1.401	1.032	.353
	26 889	58.21	2.260	1.396	1.034	.355
5	3 145	18.01	2.101	1.332	0.903	0.574
	3 428	18.32	1.973	1.342	.908	.593
	5 852	26.94	2.065	1.279	.993	.532
	6 009	26.34	2.115	1.310	.937	.551
	13 571	41.90	1.984	1.271	.947	.605
	27 184	63.85	1.873	1.204	.987	.635
	27 399	63.37	1.860	1.211	.987	.640
8	2 565	15.56	1.757	1.376	0.911	0.619
	2 669	15.79	1.753	1.366	.915	.623
	5 946	25.64	1.785	1.328	.981	.576
	6 171	25.72	1.781	1.326	.978	.581
	13 574	40.45	1.799	1.065	1.053	.698
	13 574	40.48	1.791	1.068	1.051	.700
	27 465	64.68	1.610	1.118	1.044	.716
	27 468	64.94	1.608	1.118	1.045	.714
Nozzle diameter d = 0.635 cm (0.25 in.); center-to-center nozzle spacing c_n = 2.54 cm (1 in.)						
2	2 439	16.32	3.656	1.439	0.951	-----
	2 810	19.01	3.284	1.321	.898	0.423
	6 328	32.04	3.013	1.358	.884	.344
	6 420	31.55	3.018	1.365	.885	.337
	13 075	47.52	2.709	1.282	1.005	.357
	13 084	47.44	2.718	1.288	.999	.355
	26 864	70.61	2.438	1.400	.998	.357
	26 884	71.53	2.436	1.393	.992	.355
5	2 657	18.82	3.014	1.349	0.847	0.387
	2 740	19.10	2.985	1.352	.850	.389
	6 407	30.58	2.839	1.328	.896	.398
	13 214	41.61	2.671	1.199	1.038	.402
	13 293	42.12	2.745	1.282	.970	.382

TABLE I. - Continued. HEAT-TRANSFER DATA

Dimensionless nozzle-to-target separation distance, z_n/d	Reynolds number based on nozzle diameter and nozzle exit velocity, Re_d	Average Nusselt number based on nozzle diameter, $\overline{Nu}$	Normalized local Nusselt numbers			
			$\frac{Nu_1}{\overline{Nu}}$	$\frac{Nu_2}{\overline{Nu}}$	$\frac{Nu_3}{\overline{Nu}}$	$\frac{Nu_4}{\overline{Nu}}$
5	26 875	70.28	2.350	1.309	0.987	0.443
	26 904	69.47	2.368	1.316	.983	.438
8	2 515	18.07	2.566	1.407	0.879	0.423
	2 774	18.89	2.529	1.402	.879	.436
	6 602	32.47	2.330	1.281	.991	.465
	6 619	32.55	2.324	1.283	.987	.470
	13 593	47.00	2.165	1.172	1.047	.533
	27 677	70.44	2.030	1.214	1.065	.517
Nozzle diameter d = 0.635 cm (0.25 in.); center-to-center nozzle spacing c_n = 1.27 cm (0.5 in.)						
2	2 424	21.14	2.850	1.399	0.854	0.385
	2 441	21.14	2.850	1.404	.851	.383
	6 494	36.92	2.707	1.281	.940	.423
	6 505	37.08	2.695	1.278	.942	.425
	13 091	53.02	2.477	1.279	.992	.437
	13 121	52.63	2.495	1.295	.983	.421
	30 060	70.56	2.239	1.408	.943	.442
	30 324	69.25	2.249	1.414	.944	.434
5	2 589	22.71	2.386	1.151	1.067	0.472
	2 633	22.83	2.390	1.147	1.067	.476
	6 644	40.60	2.322	1.181	1.075	.458
	6 652	40.61	2.312	1.174	1.080	.461
	12 838	61.31	2.087	1.204	1.111	.464
	13 104	61.00	2.120	1.220	1.093	.462
	21 070	75.57	1.998	1.209	1.132	.461
	29 787	79.78	1.986	1.197	1.150	.481
8	2 699	20.35	2.033	1.236	1.034	0.531
	6 590	38.39	1.911	1.148	1.144	.517
	6 628	38.28	1.914	1.149	1.143	.516
	13 064	56.36	1.748	1.109	1.192	.540
	13 155	56.24	1.777	1.116	1.176	.543
	32 695	75.81	1.704	1.135	1.131	.591
	33 012	75.06	1.705	1.137	1.131	.590

TABLE I. - Continued. HEAT-TRANSFER DATA

Dimensionless nozzle-to-target separation distance, z_n/d	Reynolds number based on nozzle diameter and nozzle exit velocity, Re_d	Average Nusselt number based on nozzle diameter, $\overline{Nu}$	Normalized local Nusselt numbers			
			$\frac{Nu_1}{\overline{Nu}}$	$\frac{Nu_2}{\overline{Nu}}$	$\frac{Nu_3}{\overline{Nu}}$	$\frac{Nu_4}{\overline{Nu}}$
Nozzle diameter d = 0.952 cm (0.375 in.); center-to-center nozzle spacing c_n = 7.62 cm (3 in.)						
2	2 577	19.63	2.199	1.458	0.887	0.469
	2 908	20.24	2.202	1.458	.880	.475
	6 040	40.65	2.117	1.462	.874	.500
	6 389	41.48	2.119	1.452	.873	.508
	13 523	63.55	2.069	1.378	.910	.539
	13 607	64.07	2.065	1.377	.909	.541
	26 820	89.28	2.014	1.362	.909	.566
	27 002	89.72	2.014	1.359	.908	.569
5	2,874	25.76	1.747	1.314	0.917	0.661
	2 942	26.68	1.743	1.304	.909	.677
	6 438	41.52	1.785	1.300	.936	.643
	6 644	41.75	1.782	1.291	.943	.644
	13 442	59.55	1.834	1.185	.985	.668
	13 593	59.63	1.848	1.187	.982	.700
	26 735	99.43	1.708	1.193	.985	.693
	26 772	98.07	1.711	1.193	.986	.692
8	2 638	22.53	1.637	1.254	0.988	0.662
	2 803	22.84	1.641	1.242	.980	.678
	6 423	37.26	1.594	1.252	.990	.673
	6 724	37.43	1.591	1.259	.989	.673
	13 457	56.53	1.572	1.176	1.022	.703
	13 663	56.70	1.571	1.170	1.023	.704
	27 174	88.06	1.481	1.091	1.074	.737
	27 190	87.59	1.483	1.092	1.077	.733
Nozzle diameter d = 0.952 cm (0.375 in.); center-to-center nozzle spacing c_n = 3.81 cm (1.5 in.)						
2	2 161	21.36	2.487	1.410	0.783	0.529
	2 345	21.71	2.496	1.415	.777	.538
	6 611	46.58	2.247	1.425	.853	.517
	6 684	46.69	2.243	1.422	.855	.517
	13 081	69.50	2.139	1.380	.903	.527
	13 132	68.65	2.150	1.386	.902	.521
	24 291	105.75	2.045	1.354	.987	.486

TABLE I. - Concluded. HEAT-TRANSFER DATA

Dimensionless nozzle-to-target separation distance, z_n/d	Reynolds number based on nozzle diameter and nozzle exit velocity, Re_d	Average Nusselt number based on nozzle diameter, $\overline{Nu}$	Normalized local Nusselt numbers			
			$\frac{Nu_1}{\overline{Nu}}$	$\frac{Nu_2}{\overline{Nu}}$	$\frac{Nu_3}{\overline{Nu}}$	$\frac{Nu_4}{\overline{Nu}}$
5	2 685	26.23	1.967	1.364	0.875	0.610
	2 705	26.22	1.969	1.362	.871	.616
	6 640	44.62	2.015	1.283	.937	.597
	6 679	44.80	2.009	1.278	.942	.598
	13 082	69.01	1.905	1.299	.956	.593
	13 126	68.86	1.903	1.302	.953	.594
	24 125	96.37	1.841	1.247	1.039	.558
	24 148	96.13	1.842	1.245	1.043	.563
8	2 805	25.49	1.729	1.240	0.947	0.691
	6 520	45.79	1.764	1.179	.998	.677
	6 570	44.80	1.774	1.180	.999	.673
	12 900	68.49	1.648	1.201	1.027	.660
Nozzle diameter d = 0.952 cm (0.375 in.); center-to-center nozzle spacing c_n = 1.905 cm (0.75 in.)						
2	2 745	29.09	2.433	1.474	0.915	0.370
	6 650	53.68	2.240	1.396	.969	.423
	6 668	53.76	2.232	1.395	.968	.428
	12 810	79.49	2.000	1.383	1.072	.390
	12 811	81.20	1.993	1.379	1.072	.395
	20 880	111.50	1.845	1.271	.962	.624
	21 155	114.50	1.836	1.259	.968	.629
5	2 687	32.07	1.958	1.377	0.976	0.503
	2 747	31.27	1.970	1.382	.977	.494
	6 658	54.50	2.014	1.310	1.015	.499
	6 672	54.12	2.021	1.309	1.015	.498
	12 490	80.47	1.918	1.292	1.056	.496
	12 492	79.48	1.927	1.292	1.055	.495
8	2 681	33.73	1.603	1.159	0.927	0.803
	2 734	33.20	1.595	1.164	.922	.807
	6 650	57.85	1.602	1.067	.971	.828
	6 780	58.33	1.595	1.065	.973	.830
	12 431	85.39	1.526	1.038	1.019	.822
	12 434	85.53	1.530	1.039	1.016	.822
	20 485	107.24	1.402	.986	1.071	.840

results of curve fitting the data in terms of equation (4) yielded the following relation:

$$\left.\begin{aligned} \frac{Nu_x}{\overline{Nu}} &= (B + 1)\left(\frac{x}{l}\right)^B \\ B &= -0.419\ Re_d^{-0.097}\left(\frac{d}{D}\right)^{-0.311}\left(\frac{c_n}{d}\right)^{0.061}\left(\frac{z_n}{d}\right)^{-0.374} \end{aligned}\right\} \quad (5)$$

Figure 6 presents Nusselt number ratios calculated from the previous relation as a function of the corresponding experimental Nusselt number ratios from table I. This figure shows the relatively large amount of scatter contained in the data. However, for a given geometrical configuration (d/D, c_n/d, and z_n/d) and Reynolds number, nearly all of the experimental Nusselt number ratios correlated quite well with the quantity $(x/l)^B$. The discrepancy between data and correlation shown in figure 6, therefore, is a result of inability to adequately describe B in terms of the dimensionless quantities d/D, c_n/d, z_n/d, and Re_d.

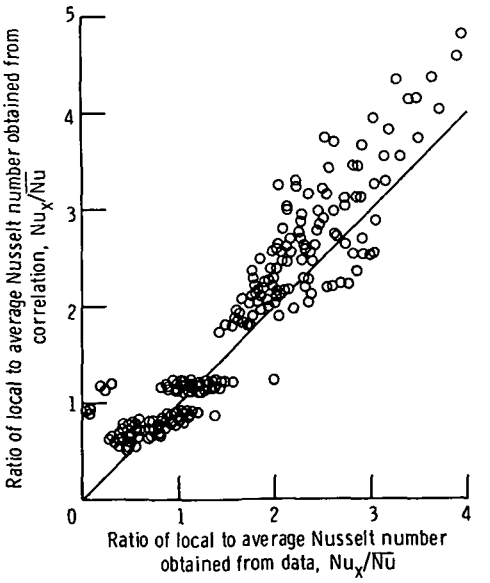

Figure 6. - Experimental Nusselt number ratio plotted against correlated Nusselt number ratio.

The effects of each of the dimensionless ratios were investigated individually by holding the remaining three fixed. The results are shown in figures 7 to 10; both experimental data and the correlation are shown in these figures.

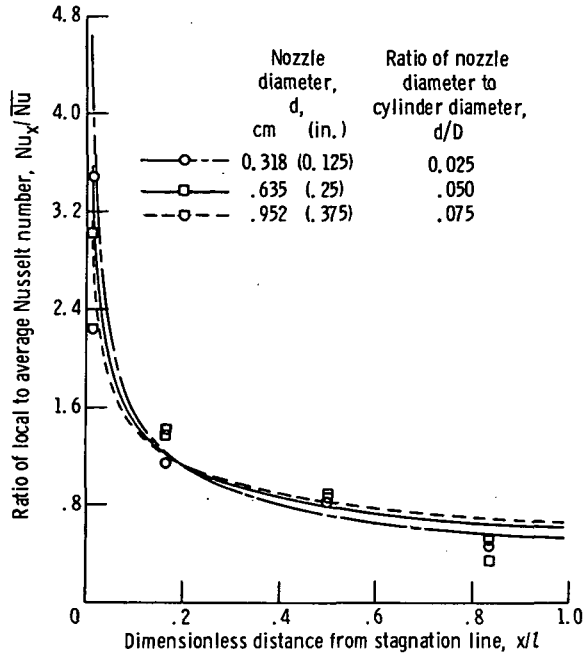

Figure 7. - Effect of ratio of nozzle diameter to cylinder diameter on normalized Nusselt number distribution. Dimensionless nozzle spacing, $c_n/d = 4$; dimensionless nozzle-to-target separation distance, $z_n/d = 2$; Reynolds number based on nozzle diameter and nozzle exit velocity $Re_d \sim 6500$. Curves from equation (5).

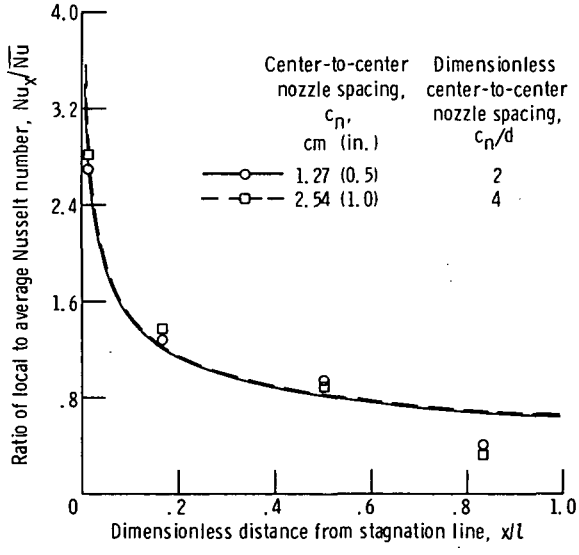

Figure 8. - Effect of ratio of center-to-center nozzle spacing to nozzle diameter on normalized Nusselt number distribution. Nozzle diameter d = 0.635 centimeter (0.25 in.); dimensionless nozzle-to-target separation distance $z_n/d = 2$; Reynolds number based on nozzle diameter and nozzle exit velocity $Re_d \sim 6500$. Curves from equation (5).

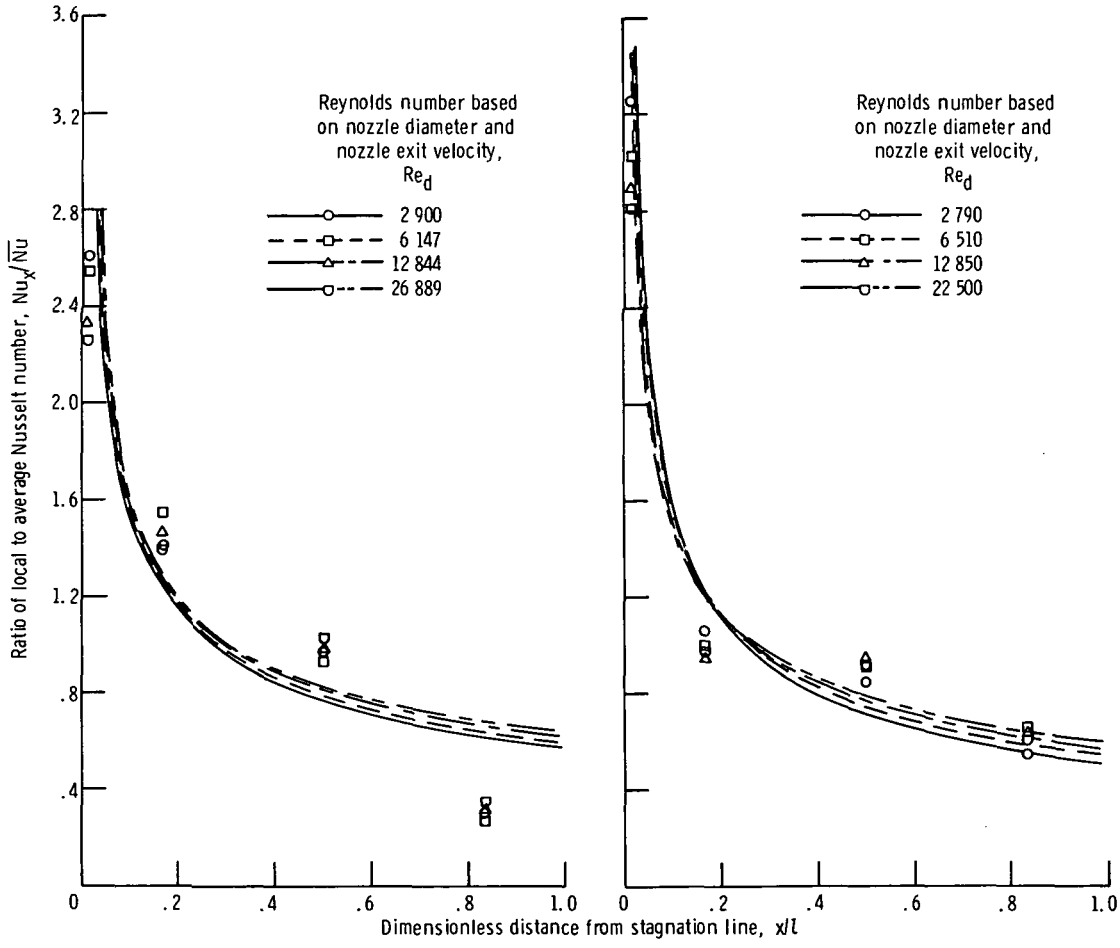

(a) Nozzle diameter d = 0.635 centimeter (0.25 in.); dimensionless nozzle-to-target separation distance z_n/d = 2; dimensionless nozzle spacing c_n/d = 8.

(b) Nozzle diameter d = 0.318 centimeter (0.125 in.); dimensionless nozzle-to-target separation distance z_n/d = 2; dimensionless nozzle spacing c_n/d = 2.

Figure 9. - Effect of Reynolds number on normalized Nusselt number distribution. Curves from equation (5).

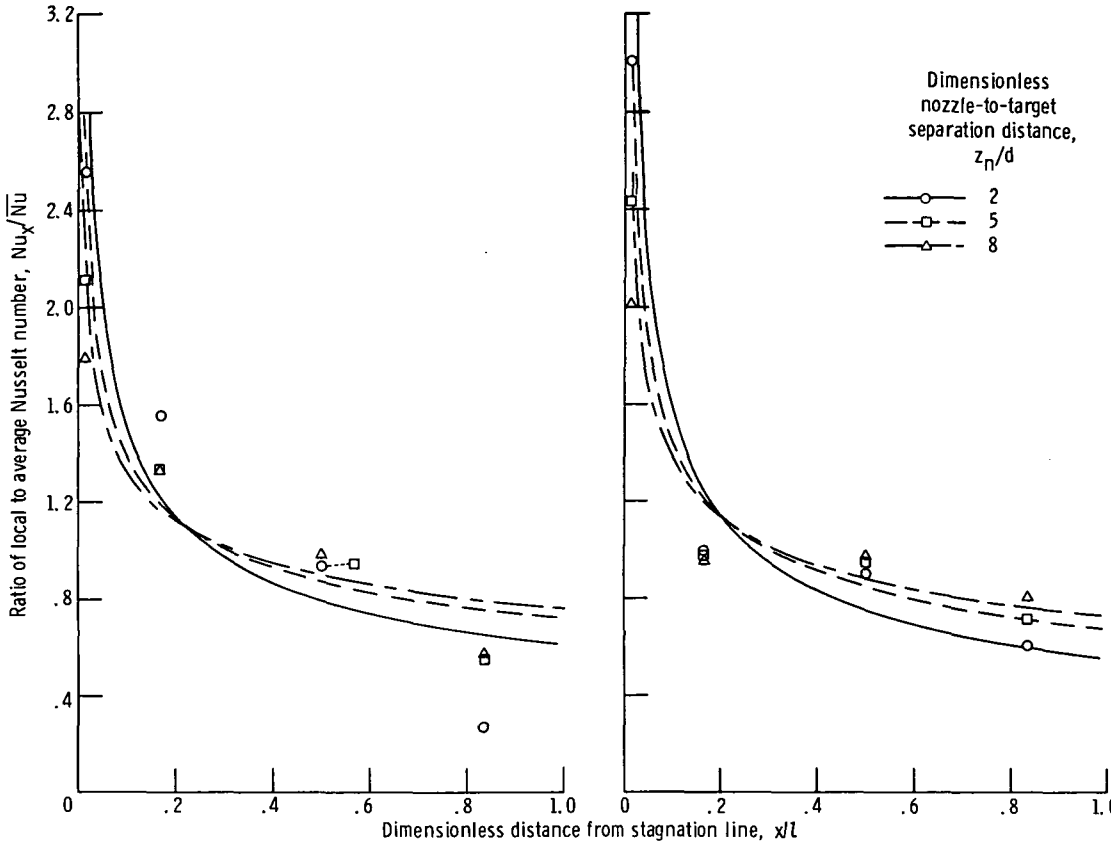

(a) Nozzle diameter d = 0.635 centimeter (0.25 in.); dimensionless nozzle spacing $c_n/d = 8$; Reynolds number based on nozzle diameter and nozzle exit velocity $Re_d \sim 6000$.

(b) Nozzle diameter d = 0.318 centimeter (0.125 in.); dimensionless nozzle spacing $c_n/d = 2$; Reynolds number based on nozzle diameter and nozzle exit velocity $Re_d \sim 6250$.

Figure 10. - Effect of ratio of nozzle to target separation distance to nozzle diameter on normalized Nusselt number distribution. Curves from equation (5).

Effect of Ratio of Nozzle Diameter to Cylinder Diameter

The effect of the ratio of nozzle diameter to cylinder diameter on the normalized Nusselt number distribution is shown in figure 7. On the figure are both the experimental and correlated normalized Nusselt number distributions for the three nozzles. Only one cylinder diameter was used in this study. The comparison was limited to the smallest of the nozzle-to-target spacings ($z_n/d = 2$) since this is the nearest to the optimum spacing reported in reference 2. The center-to-center nozzle spacing was 4 nozzle diameters, and the nozzle exit Reynolds number was approximately 6500. As was done in reference 3, the x/l value employed for the stagnation point calorimeter was one-fourth the calorimeter diameter since the maximum value would occur at the center of the stagnation point calorimeter and decrease on both sides of the stagnation line. Hence, the first x/l value considered was approximately 0.01.

Because of the way that A is defined in the expression for Nusselt number ratio $A(x/\ell)^B$, the area under each of the three curves in figure 7 must equal unity. Therefore, the curve with the highest value of Nu_x/Nu at large values of x/ℓ will have the narrowest band of peak values at small values of x/ℓ and consequently a more uniform Nusselt number distribution, as shown by the largest value of d/D, 0.075.

Effect of Ratio of Center-to-Center Nozzle Spacing to Nozzle Diameter

Figure 8 presents data for the 0.635-centimeter- (0.25-in.-) diameter nozzle located at a nozzle-to-target separation distance of 2 nozzle diameters for a nozzle exit Reynolds number of approximately 6500. Hole center-to-center spacings of 2 and 4 nozzle diameters were considered. The figure shows essentially no difference in the normalized Nusselt number distribution for the two spacing ratios.

Effect of Reynolds Number

Figure 9 shows the effects of variations in Reynolds number on the normalized Nusselt number distribution. Only two of the many possible plots of this nature are presented. Figure 9(a) presents the data for the 0.635-centimeter- (0.25-in.-) diameter nozzle with $c_n/d = 8$ and $z_n/d = 2$; figure 9(b) shows the data for the 0.318-centimeter- (0.125-in.-) diameter nozzle with $c_n/d = 2$ and $z_n/d = 2$. In both cases, except for the stagnation point, the curves show that the ratio $Nu_x/\overline{Nu}$ is practically independent of Reynolds number, a result already reported in reference 3. Figure 9(b) shows the set of data (from the 27 sets in table I) which best follows the $A(x/\ell)^B$ relation while figure 9(a) shows the set of data which deviates the most from this relation. Both the data and correlation show that the distribution becomes more uniform as Reynolds number increases.

Effect of Ratio of Nozzle-to-Target Separation Distance to Nozzle Diameter

Figure 10 presents data, for the same nozzle diameter and center-to-center spacings considered in figure 9, showing the effect of variation in the dimensionless

nozzle-to-target separation distance on the normalized Nusselt number distribution for a fixed Reynolds number. It is apparent that the nozzle-to-target separation distance has a greater effect on the normalized Nusselt number distribution than does the variation of Reynolds number. This result was previously reported in reference 3. It was also true for the other cases considered herein, even though not presented as figures.

Both the data and the set of correlation lines show that the distribution becomes flatter as the dimensionless nozzle-to-target separation distance increases. This trend seems reasonable since, as the nozzle-to-target separation distance increases, the air jet spreads. This spreading of the jet causes more of the air to impinge on the surface of the semicylinder away from the stagnation line, thus resulting in a more uniform normalized Nusselt number distribution.

Comparison of Results with Other Investigators

Information available in a number of references (refs. 3 to 7) permitted the calculation of the variation of $Nu_x/\overline{Nu}$ with x/l. Such calculations were made and the results are shown in figure 11.

Also shown in figure 11 is the distribution predicted by the experimental correlation. The distribution falls between the relatively flat distributions of references 3 and 5 and the relatively sharp distributions of references 4 and 6.

Since different ranges of variables were studied by the various investigators, it was not always possible to compare under exactly similar circumstances. Nevertheless, figure 11 indicates that reasonably good agreement exists, considering the variations in the values of z_n/d and c_n/d. Superimposed in figure 11 are a set of data obtained during the investigation reported herein. Figure 11(a) is for the case of the 0.952-centimeter (0.375-in.) nozzle with values of $c_n/d = 4$, $z_n/d = 5$, and a Reynolds number of 2685; the present data fall within the range of the results of the previous investigators. Figure 11(b) shows similar results for the 0.635-centimeter (0.25-in.) diameter nozzle for values of c_n/d and z_n/d each equal 8 and a Reynolds number of 2565.

The experimental correlation of this report for the Nusselt number ratio distribution falls approximately in the middle of the five other distributions shown in figure 11. Therefore, this correlation might be of use in obtaining the local Nusselt number in spite of the large amount of scatter in the data as shown in figure 6. However, four dimensionless ratios and five constants are needed, making use of the correlation rather cumbersome.

To facilitate usage, the correlation has been modified. The exponents on d/D and z_n/d, -0.311 and -0.374, respectively, have been averaged leaving $(d/D)^{-0.342} \times (z_n/d)^{-0.342} = (z_n/D)^{-0.342}$. The exponents on Re_d and d/c_n, -0.097 and -0.061,

Source	Dimensionless nozzle-target separation distance, z_n/d	Dimensionless nozzle spacing, c_n/d	Reynolds number based on nozzle diameter and exit velocity, Re_d
Present report	5	4	2685
Ref. 3	4.1	7.8	Not function of variable
Ref. 4	1	6.67	Not function of variable
Ref. 5	Not function of variable	Not function of variable	Not function of variable
Ref. 6	1	5	5000
Ref. 7	6	Slot jet	----

Source	Dimensionless nozzle-target separation distance, z_n/d	Dimensionless nozzle spacing, c_n/d	Reynolds number based on nozzle diameter and exit velocity, Re_d
Present report	8	8	2565
Ref. 3	7.8	7.8	Not function of variable
Ref. 4	1	6.67	Not function of variable
Ref. 5	Not function of variable	Not function of variable	Not function of variable
Ref. 6	1	8.8	5000
Ref. 7	6	Slot jet	----

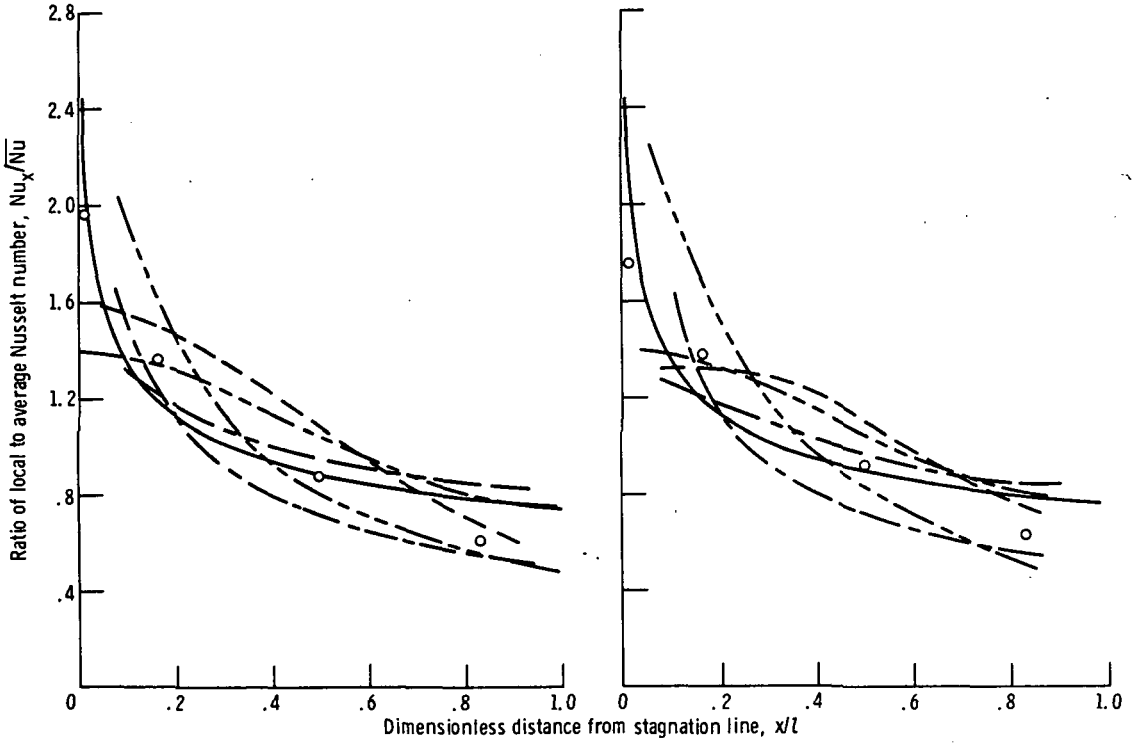

(a) Nozzle diameter d = 0.952 centimeter (0.375 in.). (b) Nozzle diameter d = 0.635 centimeter (0.25 in.).

Figure 11. - Comparison of present results with those of other investigations.

respectively, have been averaged leaving $Re_d^{-0.079}(c_n/d)^{0.079} = \left[(Gd/\mu)(d/c_n)\right]^{-0.079}$

Using these assumptions and the definition of the equivalent slot width ($b_s = \pi d^2/4c_n$) the following correlation may be obtained:

$$\frac{Nu_x}{\overline{Nu}} = (B + 1)\left(\frac{x}{l}\right)^B$$

$$B = -0.411\ Re_b^{-0.079}\left(\frac{z_n}{D}\right)^{-0.342} \tag{6}$$

Thus the four dimensionless ratios and five constants have been reduced to two dimensionless ratios and three constants.

The distribution predicted by this modified equation is shown in figure 12 for the conditions of figure 11(a) along with the original distribution as it appears in figure 11(a). The error between the original and modified correlations varies from zero at a value of $x/l = 0.24$ to about 15 percent at a value of $x/l = 1$. For values of $x/l < 0.24$, the modified correlation overestimates the value of $Nu_x/\overline{Nu}$; for values of $x/l > 0.24$, the modified correlation underestimates the value of $Nu_x/\overline{Nu}$. It should be noted that, although the modified correlation has a term containing the diameter of the target cylinder, only one value of this diameter was used throughout the test program. If this modified correlation is considered satisfactory, it can then be used in conjunction with the average Nusselt number correlation recommended in reference 1 to determine the Nusselt number distribution along the cooled surface length of a semicylindrical surface such as the leading edge of a turbine blade.

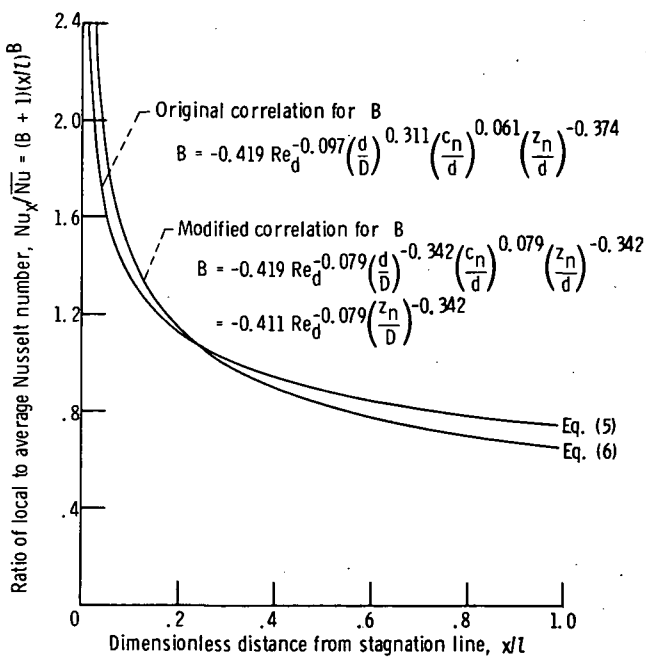

Figure 12. - Comparison of original experimental correlation with modified experimental correlation. Ratio of nozzle diameter to cylinder diameter $d/D = 0.05$; dimensionless nozzle-to-target separation distance $z_n/d = 8$; dimensionless nozzle spacing $c_n/d = 8$; Reynolds number based on nozzle diameter and nozzle exit velocity $Re_d = 2565$.

SUMMARY OF RESULTS

The results of an experimental study of the local heat-transfer characteristics of a row of turbulent air jets impinging on a concave semicylindrical surface are as follows:

1. A correlation for expressing the ratio of local to average Nusselt number over the cooled concave surface is presented.

2. The experimental data and the correlation are compared with available distributions in the literature. The results of the investigation reported herein were found to approximate the average of those in the literature.

3. Of four dimensionless ratios (c_n/d, Re_d, d/D, and z_n/d) studied, the effects on the normalized Nusselt number distribution of d/D and z_n/d were significant; the effects of c_n/d and Re_d on the distribution were not significant.

4. For ease in application, an approximation to the correlation which considers only Re_b and z_n/D as independent variables was obtained.

Lewis Research Center,
National Aeronautics and Space Administration,
Cleveland, Ohio, October 4, 1972,
501-24.

REFERENCES

1. Livingood, John N. B.; and Gauntner, James W.: Average Heat-Transfer Characteristics of a Row of Circular Air Jets Impinging on a Concave Surface. NASA TM X-2657, 1972.

2. Metzger, D. E.; Yamashita, T.: and Jenkins, C. W.: Impingement Cooling of Concave Surfaces with Lines of Circular Air Jets. J. Eng. Power, vol. 91, no. 3, July 1969, pp. 149-158.

3. Chupp, Raymond E.; Helms, Harold E.; McFadden, Peter W.; and Brown, Tony R.: Evaluation of Internal Heat-Transfer Coefficients for Impingement-Cooled Turbine Airfoils. J. Aircraft, vol. 6, no. 3, May-June 1969, pp. 203-208.

4. Jenkins, C. W.: and Metzger, D. E.: Local Heat Transfer Characteristics on Concave Cylindrical Surfaces Cooled by Impinging Slot Jets and Lines of Circular Jets with Spacing Ratios 1.25 to 6.67. Tech. Rep. ME-694, Arizona State Univ., May 1969.

5. Jusionis, Vytautas J.: Heat Transfer from Impinging Gas Jets on an Enclosed Concave Surface. J. Aircraft, vol. 7, no. 1, Jan.-Feb. 1970, pp. 87-88.

6. Tabakoff, W.; and Clevenger, W.: Gas Turbine Blade Heat Transfer Augmentation by Impingement of Air Jets Having Various Configurations. J. Eng. Power, vol. 94, no. 1, Jan. 1972, pp. 51-60.

7. Burggraf, F.: Local Heat Transfer Coefficient Distribution with Air Impingement into a Cavity. Paper 72-GT-59, ASME, Mar. 1972.

NASA-Langley, 1972 — 33 E-7117

NATIONAL AERONAUTICS AND SPACE ADMINISTRATION
WASHINGTON, D.C. 20546

OFFICIAL BUSINESS
PENALTY FOR PRIVATE USE $300

SPECIAL FOURTH-CLASS RATE BOOK

POSTAGE AND FEES PAID
NATIONAL AERONAUTICS AND SPACE ADMINISTRATION
451

U.S.MAIL

POSTMASTER: If Undeliverable (Section 158 Postal Manual) Do Not Return

"The aeronautical and space activities of the United States shall be conducted so as to contribute . . . to the expansion of human knowledge of phenomena in the atmosphere and space. The Administration shall provide for the widest practicable and appropriate dissemination of information concerning its activities and the results thereof."

—NATIONAL AERONAUTICS AND SPACE ACT OF 1958

NASA SCIENTIFIC AND TECHNICAL PUBLICATIONS

TECHNICAL REPORTS: Scientific and technical information considered important, complete, and a lasting contribution to existing knowledge.

TECHNICAL NOTES: Information less broad in scope but nevertheless of importance as a contribution to existing knowledge.

TECHNICAL MEMORANDUMS: Information receiving limited distribution because of preliminary data, security classification, or other reasons. Also includes conference proceedings with either limited or unlimited distribution.

CONTRACTOR REPORTS: Scientific and technical information generated under a NASA contract or grant and considered an important contribution to existing knowledge.

TECHNICAL TRANSLATIONS: Information published in a foreign language considered to merit NASA distribution in English.

SPECIAL PUBLICATIONS: Information derived from or of value to NASA activities. Publications include final reports of major projects, monographs, data compilations, handbooks, sourcebooks, and special bibliographies.

TECHNOLOGY UTILIZATION PUBLICATIONS: Information on technology used by NASA that may be of particular interest in commercial and other non-aerospace applications. Publications include Tech Briefs, Technology Utilization Reports and Technology Surveys.

Details on the availability of these publications may be obtained from:

SCIENTIFIC AND TECHNICAL INFORMATION OFFICE

NATIONAL AERONAUTICS AND SPACE ADMINISTRATION

Washington, D.C. 20546